Numerical Analysis of Time-gated Confocal Microscopy through Anisotropically Scattering Media

Marcus Magnor
Stanford University, Computer Graphics Laboratory, Stanford, CA 94305
phone 650-723-3154, fax 650-723-0033, magnor@graphics.stanford.edu
Wolfgang Rudolph
University of New Mexico, Dept. Physics and Astronomy, Albuquerque, NM 87131

Abstract: An efficient and fast simulation technique is used to calculate the confocal imaging contrast through anisotropically scattering media when time-gating techniques are applied. Optimal time-gate width is found to depend on object reflection characteristics, and forward-scattering media enhance imaging contrast only for non-absorbing objects.

OCIS codes: 000.4430, 170.1790, 170.3660, 170.7050, 170.6920, 290.4210

Confocal microscopy is an established imaging technique in biology and medicine. Its inherent depth discrimination characteristics permit non-invasive examination of objects buried under scattering layers. With increasing penetration depth, however, the image contrast degrades due to light scattered outside the focal region. Time-gating techniques can efficiently reject those stray light components that exhibit total optical path lengths different from the light scattered inside the focal region [7]. In order to optimize the optical parameters of confocal imaging systems for microscopy through scattering layers with and without time gates, it is necessary to develop theoretical models. While the limiting cases of single scattering [2] and diffusion [4] can be analytically modeled, no closed-form expression has yet been found to describe multiple scattering in combination with imaging optics. *Monte Carlo (MC)*-based computer algorithms have been developed to simulate light propagation through random scattering media [1, 8]. Unfortunately, time-consuming simulations are necessary to obtain statistically reliable results when applying MC methods directly to confocal microscopy [5]. To improve statistics and shorten simulation time, the MC simulation can be biased to assign more weight to photons that reach the detector [6]. While biased MC simulation has been shown to predict confocal imaging characteristics with acceptable computational effort, its accuracy degrades if the pinhole size approaches the confocal limit. We present an efficient simulation technique for confocal imaging through scattering materials based only in parts on MC simulation that enables predicting imaging contrast and lateral resolution when time gates are applied [3]. The simulation accuracy is independent of the pinhole diameter and scatter density, yielding reliable predictions for dense scatterers and true confocal imaging. In this work, simulation results are presented for imaging different types of objects through anisotropically scattering media.

To examine confocal microscopy through scattering media, the response of the optical system and the propagation of light through the scatterer must be modeled correctly. The scattering medium itself is considered as a slab of infinite thickness with scattering properties defined by the scattering coefficient μ and the anisotropy parameter g. The simulation is based on the schematic diagram depicted in Fig. 1a. The optical system is treated in the approximation of geometrical optics which has been shown to realistically describe depth discrimination properties and contrast behavior of confocal microscopy [5, 6]. The function $P(r,z)$ describes the probability of a photon scattered at a depth z and radial location r to pass through the pinhole and to contribute to the detected signal. It is nonzero only within a confined volume, defined by a radius $R(z)$, which is referred to as the *active volume*. Light scattered outside this active volume does not contribute to the detected signal unless an additional scattering event takes place. $P(r,z)$ peaks sharply in the focal plane, $z=d$, and decreases with increasing distance from the focus. The active volume is subdivided into volume elements (voxels). The voxels have to be small enough such that $P(r,z)$ can be assumed constant within each volume element. Small voxels are required around the focal region, while the voxel size can be gradually increased towards the surface. The axial symmetry suggests voxels that have the shape of partial annuli, cf. Fig. 1a, with size parameters Δr, Δz, and $r\Delta\alpha$. The total number of voxels in the active volume depends on focus depth d as well as on the numerical aperture NA. For a scattering volume extending to infinity along the optical axis, the active volume is also infinitely large. However, for scattering densities $\mu d \geq 1$, as

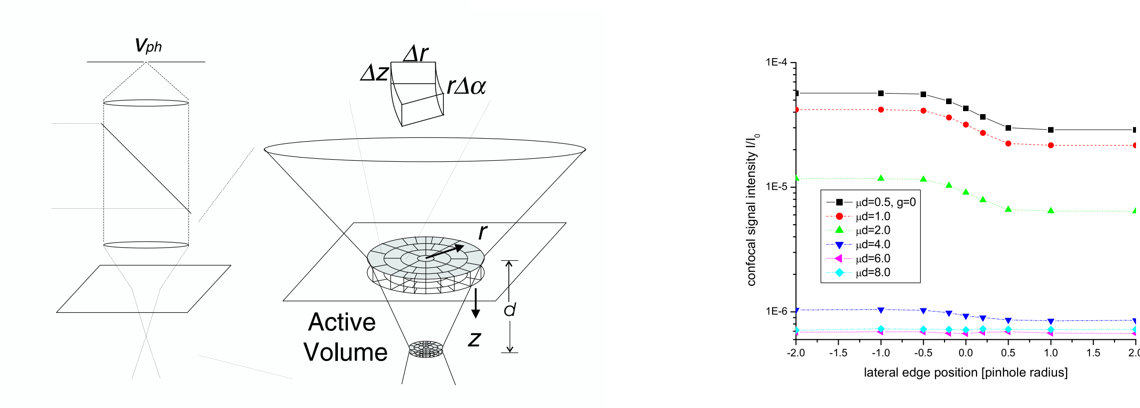

(a) (b)

Fig. 1. (a) Schematic diagram of confocal imaging through scattering layers. The volume region from which light can be scattered into the pinhole is subdivided into voxels. (b) Confocal signal when moving a totally absorbing edge through focus for different scattering densities and isotropic scattering (g=0). The edge touches the active volume at -1 and covers the entire focus at +1.

examined here, it is sufficient to extend the active volume to twice the distance from the surface to the focal plane [3].

The simulation divides the photons into three groups – singly scattered photons, doubly scattered photons, and multiply scattered photons, whose probabilities to reach the detector are calculated separately and summed in the end. The contribution of singly scattered light to the detected signal can be precisely determined. The intensity of un-scattered light is known to decrease exponentially with z, and for each voxel the amount of light being scattered into the pinhole $P(r, z)$ is calculated. Since the directly illuminated volume is identical to the active volume from which light can be scattered into the pinhole, for doubly scattered light to reach the detector, both scattering events must lie within the active volume. All combinations of voxels must be considered, with one voxel scattering a fraction of the illuminating light to a second voxel which in turn scatters part of that light into the pinhole. In order to describe the influence of light that is scattered three and more times, a refined Monte Carlo simulation technique [8] is applied in conjunction with the above-described discretized active-volume approach [3]. The Monte-Carlo simulation traces random photon paths through the scatterer. At each scattering location, the photon's probability to reach each active-volume voxel, and on from there to reach the pinhole, is calculated. In previous MC-based simulations, photons had to reach the pinhole by chance. Thus, the number of necessary photon trajectories had to increase with decreasing pinhole diameter to obtain statistically reliable predictions [5, 6]. In contrast, in our simulation all considered photon paths end in the pinhole and are weighted according to their individual probability. The prediction accuracy is thus independent of pinhole size and scattering density. The simulation further allows one to describe the propagation and scattering of light pulses. By referring the photon paths to a common reference, path lengths can be converted to arrival time differences at the pinhole.

Fig. 1b depicts the confocal response without time gating when a totally absorbing edge is moved through focus in lateral direction. With increasing optical thickness μd, the signal steepness decreases, until no difference can be perceived anymore. In the following, the confocal imaging contrast is defined as

$$c = \frac{|I_{\text{left}} - I_{\text{right}}|}{I_{\text{left}} + I_{\text{right}}}$$

where I_{left} is the confocal signal when the object's edge is far away from the focus, and I_{right} denotes the detected signal when the planar object covers the entire focal plane. The contrast c ranges from 0 to 1, where 1 signifies the maximum possible contrast, and 0 denotes the loss of all imaging contrast. For the presented simulation results, the numerical aperture is set to $NA = 0.4$, the pinhole has a diameter of 2 optical units (corresponding to true confocal imaging), the focus is located $f = 0.5$mm below the scattering medium's surface, and the illumination pulse is 10fs long. The scattering medium's optical thickness is stated as the mean number of scattering events from medium surface to focus, μd. Fig. 2a depicts the

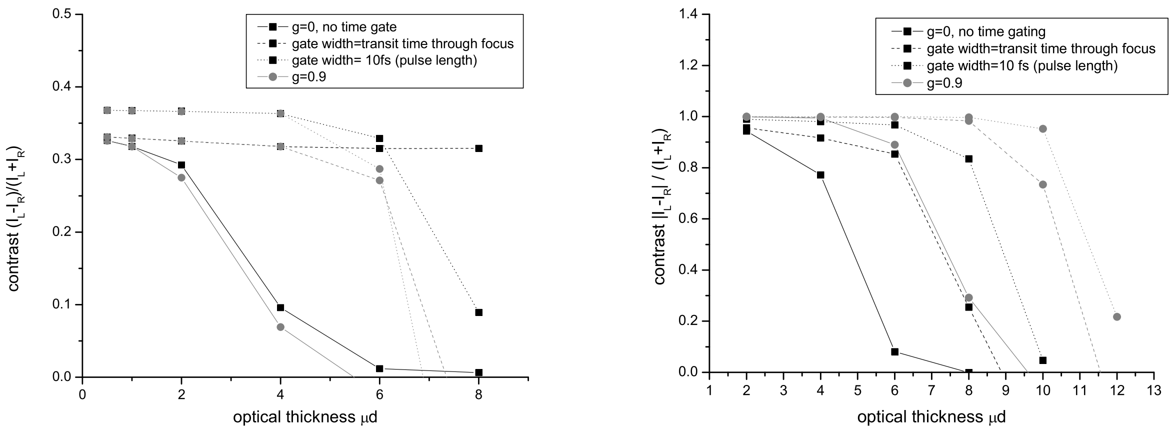

(a) Absorbing object (b) Lambertian object

Fig. 2. Imaging contrast for a totally absorbing object (a) and an isotropically scattering Lambertian object (b). Time-gating increases optical depth range, whereas anisotropic scattering enables deeper penetration only for non-absorbing targets.

imaging contrast of a completely absorbing object assuming an isotropic (g=0) and an anisotropic (g=0.9) scattering medium. With increasing optical thickness, contrast degrades equally for isotropic and anisotropic scattering surroundings, because the additional 'snake light', i.e. forward-scattered photons that stay close to the ballistic path, reaching the focus in case of forward scattering (g=0.9) is absorbed and does not enhance the signal from the focus region. When time-gating techniques are applied, imaging contrast remains constant up to higher optical thicknesses, and imaging through denser scattering media becomes possible. A time-gate width equal to the extent of the focal region along the optical axis appears to yield better results than time-gating with the duration of the illumination pulse (10fs). In Fig. 2b, the imaging contrast of a Lambertian object (isotropically, diffusely reflecting surface) is shown. For non-absorbing objects, anisotropic scattering (g=0.9) yields better imaging characteristics, as the additional 'snake light' reaching the focus is now (diffusely) reflected back into the medium and may contribute to the signal. Time-gating extends the range of penetrable optical thickness, while now a time-gate width matched to the illumination pulse length yields optimal imaging characteristics.

In summary, the effect of scattering anisotropy and the width of the optimum time gate depend on the optical properties of the structure to be imaged.

References

1. S.T. Flock, M.S. Patterson, B.C. Wilson, and D.R. Wyman. Monte carlo modeling of light propagation in highly scattering tissue-I: Model predictions and comparison with diffusion theory. *IEEE Trans. on Biomedical Engineering*, 36(12):1162–1167, 1989.
2. M. Kempe, A.Z. Genack, W. Rudolph, and P. Dorn. Ballistic and diffuse light detection in confocal and heterodyne imaging systems. *J. Opt. Soc. Am. A*, 14(1):216–223, 1997.
3. M. Magnor, P. Dorn, W. Rudolph, Simulation of confocal microscopy through scattering media with and without time gating. *J. Opt. Soc. Am. B*, 18(11):1695–1700, 2001.
4. M.S. Patterson, B. Chance, and B.C. Wilson. Time resolved reflectance and transmittance for the non-invasive measurement of tissue optical properties. *Appl. Opt.*, 28(12):2331–2336, 1989.
5. J.M. Schmitt, A. Knüttel, and M. Yadlowsky. Confocal microscopy in turbid media. *J. Opt. Soc. Am. A*, 11(8):2226–2235, 1994.
6. J.M. Schmitt and K. Ben-Letaief. Efficient monte carlo simulation of confocal microscopy in biological tissue. *J. Opt. Soc. Am. A*, 13(5):952–961, 1996.
7. J.M. Schmitt. Optical coherence tomography (OCT): A review. *IEEE J. Sel. Top. Quantum Electronics*, 5(4):1205–1215, 1999.
8. E. Tinet, S. Avrillier, and J.M. Tualle. Fast semianalytical monte carlo simulation for time-resolved light propagation in turbid media. *J. Opt. Soc. Am. A*, 13(9):1903–1915, 1996.